Analysis and Optimization of Cutting Forces in the Hard Turning of 90CrSi Steel using Al_2O_3 NFMQL

MINH TUAN NGO
Department of Manufacturing Engineering, Faculty of Mechanical Engineering, Thai Nguyen University of Technology, Thai Nguyen 250000,
VIETNAM

Abstract: This study focuses on the analysis and optimization of technology parameters for the Nanofluid Minimum Quantity Lubricationmethod in the hard turning of 90CrSi steel. The effects of Al_2O_3 nanoparticle concentration (NC), air pressure (p) and air flow rate (Q) on the active cutting force (F_a), passive cutting force (F_p), and specific cutting force (P_{c-c}) were analyzed by an experimental study. The results showed that NC&p were the factors that greatly affected Fa and Pc−c. F_a and P_{c-c} reached small values at low concentrations and medium pressure levels (about 5.2 Bar). In contrast, F_p is strongly influenced by the interaction between factors and reached a minimum value at 4.0 Bar. Furthermorea multi-objective optimization method was used to find a compromise solution. The overall optimal parameters proposed were: NC≈0.79%, p≈4.97 Bar, and Q≈205.6 l/min. This result provides suitable technological parameters, while also improving cutting efficiency and machining accuracy in real-world manufacturing applications.

Key-Words: NFMQL, hard turning, nanofluids, cutting force, lubricant, CBN, Al_2O_3, Optimization

Received: March 24, 2025. Revised: July 27, 2025. Accepted: August 29, 2025. Published: May 27, 2026.

1 Introduction

In machining, some materials such as hardened steel, titanium alloys and nickel-based superalloys often cause great difficulties in cutting, due to large cutting forces, high cutting temperatures, excessive tool wear and affected surface integrity. Through the analysis of the machining mechanism of hard metals, several cooling and lubrication techniques have been proposed to solve problems of cutting temperature and tool wear [1]. At the same time, many integrated research techniques involving experimentation, modeling, and optimization have also been carried out in the study of machinability analysis using combined lubrication methods [2].

In recent years, Minimum Quantity Lubrication (MQL) has emerged as a promising sustainable machining method, capable of significantly reducing coolant usage while maintaining lubrication and cooling [3], [4], [5]. These studies mainly focus on researching cutting fluids, optimizing nozzle structure, and using cutting fluids supplemented with nanoparticles. The results showed superior performance in reducing cutting temperatures and tool wear when nanoparticles were used. MQL using nano-solutions has received considerable attention due to its ability to enhance thermal conductivity, improve lubricity, and prolong tool life [6], [7], [8].

These studies have shown the role of nanoparticles such as MoS_2, Al_2O_3, and graphene in improving surface quality and increasing wear resistance due to enhanced friction properties. Simultaneously, studies have demonstrated that nanofluid solutions can reduce cutting forces and improve lubrication during the machining of titanium alloys used in medical applications. Furthermore, the results have identified that hybrid nanofluids exhibit superior thermal conductivity and stability compared to single-particle suspensions, indicating their suitability for high-performance machining applications.

The application of nano-MQL in cutting hard machine alloys has shown promising results. Tool life is improved, and workpiece morphology is favorable when machining Inconel 718 with nano-cutting fluids, due to reduced adhesion and better heat dissipation [9]. The machinability of Inconel 718 can also be improved by selecting new cutting tools with appropriate lubrication and cooling conditions [10]. Furthermore, the application of vegetable oil mixed with nanoparticles could be an effective solution for machining Inconel 800 [11]. Using vegetable oil has the potential to improve lubrication and reduce environmental impact compared to mineral oil-based fluids. In particular, MoS_2 -based nanofluids have attracted the attention of many researchers due to their solid-based lubricating properties. MoS2 particles, with their layered structure, when mixed with vegetable oil, create a solid lubricating film in the cutting zone, reducing cutting force and improving surface finish during the grinding process with the MQL method [12]. The TOPSIS method was combined with ANOVA to determine suitable finishing milling parameters when machining Ti-6Al-4V alloys with MQL [13]. A process to improve surface integrity and machining performance for difficult-to-machine materials was also proposed. The effectiveness of using MQL with nano-solutions has also been demonstrated when machining other materials such as martensite stainless steel, AA 2024 T3 aluminum alloy [14], [15] and [16]. The results of studies also show that the use of MoS_2 nano-lubricants in machining can improve surface morphology and reduce chip adhesion to cutting tools. Coconut oil mixed with Al2O3 particles not only has superior cooling and lubrication performance when machining conventional AISI 1040 steel but is also environmentally friendly [17]. Nanofluid applications in Inconel 617 turning processes are also studied using multi-objective optimization models to simultaneously minimize cutting force, surface roughness, and tool wear [18]. Furthermore, hybrid nanofluids by combining two types of graphene and Al_2O_3 nanoparticles also show superior friction properties in high-precision grinding of difficult-to-machine materials [19]. In addition to the type of fluid, the design of the MQL system plays an important role in the cooling and lubrication performance of the MQL [20]. The size and density of droplets during MQL machining also significantly impact the machining processes. Research results show that smaller, more evenly dispersed droplets improved lubrication and cooling efficiency due to enhanced penetration into the cutting zone.

Overall, recent studies [3], [4] indicate that nano-MQL—when combined with optimized fluid formulations and precise dispensing systems—offers a highly efficient, environmentally friendly solution for machining hard and aerospace-grade materials.

While recent researches confirm the significant benefits of nanofluid MQL (NFMQL) technology when machining a variety of materials, there remains a significant research gap when it comes to the application and systematic optimization of NFMQL parameters for hard turning of high-strength die steels, such as 90CrSi. Furthermore, while individual performance metrics such as tool wear and surface roughness have been extensively studied, a comprehensive analysis of the individual cutting force components – active (F_a), passive (F_p), and specific ($P_{c\text{–}c}$) – as well as the requirements for simultaneous optimization of these objectives, is also lacking.

The interactive effects of NFMQL technological parameters such as nanoparticle concentration, air pressure, and flow rate have not been analyzed for this specific application. Studies have mainly focused on optimizing MQL parameters for titanium alloys using TOPSIS and ANOVA, or investigating the effects of MoS_2, Al_2O_3, and Graphene nanoparticles in machining processes. Therefore, the research focusing on the simultaneous optimization of three separate cutting force components (active, passive, and specific) in hard turning of 90CrSi using NFMQL Al_2O_3 technology is still an open field. Therefore, this study conducts a comprehensive investigation on the effects of Al_2O_3 nanoparticle concentration (NC), air pressure (p), and flow rate (Q) on the active cutting force, passive cutting force, and specific cutting force in hard turning of 90CrSi steel. The main objective is to analyze the main and interactive effects of the studied parameters on the objective functions and perform multi-objective optimization to determine a set of optimal parameters for the NFMQL Al_2O_3 method, applied in hard turning of 90CrSi steel.

2 Experimental system and method

In this study, a series of experiments was conducted to investigate the influence of different parameters on the cut parts during hard turning using minimum quantity lubrication (MQL) with Al_2O_3 nanofluid. By varying the nanoparticle concentration, air pressure, and air flow rate, this study aimed to analyze the influence level and trend of NFMQL process parameters on the specific cutting force, active cutting force, and passive cutting force during hard turning under MQL conditions. The experimental model is illustrated in Figure 1. The experiments were carried out on a CS-460x1000 Chu Shing lathe (manufactured by Pin Shin Machinery Company). All workpieces used in the experiments were made of 90CrSi steel, with dimensions of D40xL200, and were hardened to the hardness range of 60-62 HRC.

The experiments utilized CBN inserts (CCGW09T308S01020FWH7025) manufactured by Sandvik, along with an MQL nozzle from the NOGA brand. For the nanofluid preparation, aluminum oxide (Al_2O_3) nanoparticles with a purity of 99.5%+ and a size of 30 nm were added to a vegetable-based cutting oil (Rice oil) in varying concentrations of 0.5%, 1%, and 1.5%.

DOI: 10.37394/232011.2026.21.5

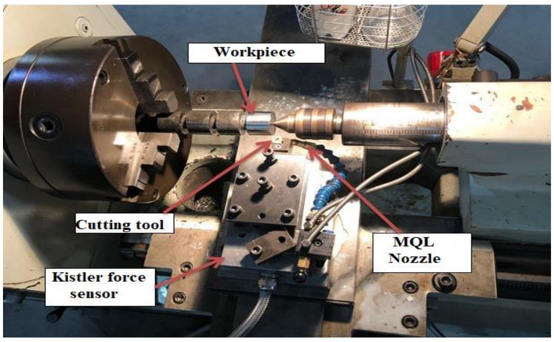

Fig. 1: *Experiment setup.*
"Source: Created by authors"

During the cutting process, a Kistler 9257BA dynamometer (Germany) with A/D data collection and Dasylab 10.0 software was employed to measure the three components of cutting force (F_f, F_p, F_c), Figure 2. To evaluate machinability, in addition to utilizing the three components of the cutting force, the active and passive cutting forces are also commonly used. The passive force (F_p), which corresponds to the thrust force on the workpiece, is a cause of machining inaccuracy. Meanwhile, the active cutting force (F_a) is synthesized from the main cutting force (F_c) and the feed force (F_f) according to the following formula (1): $F_a = \sqrt{F_c^2 + F_f^2}$ (1)

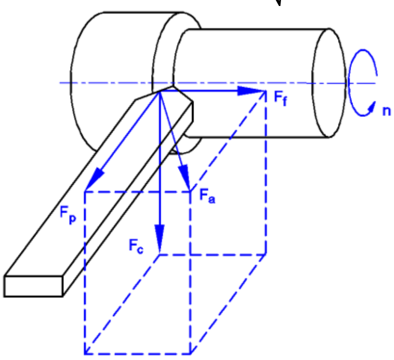

Fig. 2: *Cutting forces in the turning process.*
"Source: Created by authors"

Simultaneously, to evaluate chip formation capability during the machining process, this paper utilizes the specific cutting force as the objective function. The specific cutting force represents the force required to remove a chip, calculated per square millimeter of chip cross-sectional area. The specific cutting force is determined by the following equation (2): $P_{c-c} = \frac{F_c}{f.d}$ (N/mm^2) (2)

In this study, based on the manufacturer's recommendations and previous publications, the cutting parameters were always maintained in all experiments: V=160m/min; f=0.12 mm/rev; d=0.12mm. The study evaluates the influence of NF MQL parameters (NC nanoparticle concentration, air pressure p, and air flow Q) on the specific cutting force (P_{c-c}), the active and passive (F_a and F_p). Input parameters and their corresponding values were determined by considering both the experimental equipment's capacity and the findings of prior research [3], [4]. These selected parameters, essential for the study, are detailed in Table 1.

Table 1. *Survey parameters and value levels*

No.	Parameters	Symbols	Low	High
1	Nanoparticle concentration (%)	NC	0,5	1,5
2	Air pressure (Bar)	p	4	6
3	Air flow (l/min)	Q	150	250

"Source: Created by authors"

Table 2. *Experimental matrix and results*

Std.	Run	NC (%)	P (Bar)	Q (l/min)	Fp (N)	Fc (N)	Ff (N)	Fa (N)	Pc-c (N/mm2)
1	1	0.5	4	200	157.0	100.5	28.7	104.5	6977.8
11	2	1	4	250	105.6	92.5	27.5	96.5	6425.7
7	3	0.5	5	250	171.0	110.4	29.6	114.3	7668.1
6	4	1.5	5	150	145.9	94.8	23.8	97.7	6581.9
14	5	1	5	200	109.9	92.2	28.9	96.6	6402.1
15	6	1	5	200	118.9	98.5	30.1	103.0	6838.2
3	7	0.5	6	200	248.0	116.6	26.3	119.6	8100.0
12	8	1	6	250	262.0	122.0	25.7	124.7	8470.8
2	9	1.5	4	200	135.4	115.8	19.4	117.4	8043.1
8	10	1.5	5	250	236.8	121.8	28.1	125.0	8461.1
4	11	1.5	6	200	266.8	130.5	30.3	134.0	9064.6
10	12	1	6	150	213.3	111.0	12.1	111.6	7707.6
9	13	1	4	150	230.6	134.7	30.6	138.1	9354.2
5	14	0.5	5	150	280.8	148.9	27.4	151.4	10337.5
13	15	1	5	200	188.0	113.1	26.4	116.2	7856.9

"Source: Created by authors"

The Box-Behnken method is used to build an experimental planning diagram for the influence of nanoparticle concentration (NC), Pressure (p) and flow (Q) on the specific cutting force, the active and passive (F_a and F_p), as shown in Table 2. This study uses Minitab 21 software to design experimental plans and conduct experiments in running order (RunOrder).

3 Results and discussion

3.1 Analysis of Variance for Specific Cutting Force and Cutting Force Components

To evaluate the level of influence of the input process parameters (NC, p, Q) and their second-order interactions on the investigated responses (P_{c-c}, F_a, F_p), an Analysis of Variance (ANOVA) was performed on the dataset collected from the Box-Behnken design matrix. The ANOVA results for the investigated factors are presented in Table 3, Table 4, and Table 5. As summarized in Table 3, the statistical analysis results show the effect of the cutting parameters on the specific cutting force. Similarly, in Table 4, the results of the statistical analysis regarding the effect of the cutting parameters on the active cutting force are summarized. And the results of the analysis of variance for the passive cutting force are also shown in Table 5.

Table 3. *Results of the analysis of variance for the specific cutting force*

Source	DF	Adj SS	Adj MS	F-Value	P-Value
Model	9	14664772	1629419	2.22	0.197
Linear	3	9375138	3125046	4.26	0.076
NC (%)	1	5007294	5007294	6.82	0.048
p (Bar)	1	4256511	4256511	5.8	0.061
Q(l/min)	1	111333	111333	0.15	0.713
Square	3	3047501	1015834	1.38	0.35
NC*NC	1	803305	803305	1.09	0.343
p*p	1	2441321	2441321	3.33	0.128
Q*Q	1	25180	25180	0.03	0.86
2-Way interac.	3	2242133	747378	1.02	0.458
NC*p	1	1361921	1361921	1.86	0.231
NC*Q	1	837098	837098	1.14	0.334
p*Q	1	43114	43114	0.06	0.818
Error	5	3670881	734176		
Lack-of Fit	3	1079244	359748	0.28	0.841
Pure Error	2	2591636	1295818		
Total	14	18335652			

"Source: Created by authors"

The results indicate that the first-order effect of pressure (p) on the specific cutting force, active cutting force, and passive cutting force is significant, but the second-order interaction effect of air pressure is less significant. While the main effect of the NC particle concentration is significant for the specific cutting force and the active cutting force, it has little influence on the passive cutting force. The interactions NC(%)*Q(l/min) and p(Bar)*Q(l/min) have a strong influence on the passive cutting force.

Table 4. *Results of the analysis of variance for the active cutting force*

Source	DF	Adj SS	Adj MS	F-Value	P-Value
Model	9	2949	327.67	2.37	0.178
Linear	3	1957.3	652.43	4.71	0.064
NC (%)	1	1085.46	1085.46	7.84	0.038
p (Bar)	1	855.33	855.33	6.18	0.055
Q (l/min)	1	16.52	16.52	0.12	0.744
Square	3	568.07	189.36	1.37	0.353
NC* NC	1	145.23	145.23	1.05	0.353
p* p	1	456.16	456.16	3.3	0.129
Q* Q	1	16.72	16.72	0.12	0.742
2-Way Interac.	3	423.63	141.21	1.02	0.458
NC* p	1	244.24	244.24	1.76	0.241
NC*Q	1	174.88	174.88	1.26	0.312
p*Q	1	4.51	4.51	0.03	0.864
Error	5	691.98	138.4		
Lack-of-Fit	3	185.94	61.98	0.24	0.861
Pure Error	2	506.04	253.02		
Total	14	3640.98			

"Source: Created by authors"

Table 5. *Results of the analysis of variance for the passive cutting force*

Source	DF	Adj SS	Adj MS	F-Value	P-Value
Model	9	46527	5169.7	4.72	0.051
Linear	3	18106.6	6035.5	5.51	0.048
NC (%)	1	645.8	645.8	0.59	0.477
p (Bar)	1	16327.1	16327.1	14.9	0.012
Q (l/min)	1	1133.6	1133.6	1.03	0.356
Square	3	10407.9	3469.3	3.17	0.123
NC*NC	1	4342.9	4342.9	3.96	0.103
p *p	1	3013.5	3013.5	2.75	0.158
Q*Q	1	4627.9	4627.9	4.22	0.095
2-Way Interac.	3	18012.5	6004.2	5.48	0.049
NC*p	1	408.2	408.2	0.37	0.568
NC*Q	1	10063.1	10063.1	9.19	0.029
p *Q	1	7541.2	7541.2	6.88	0.047
Error	5	5477.8	1095.6		
Lack-of-Fit	3	1829.1	609.7	0.33	0.807
Pure Error	2	3648.7	1824.3		
Total	14	52004.8			

"Source: Created by authors"

3.2 Influence on the Specific Cutting Force

The main effects of the factors on the specific cutting force are illustrated in Figure 3. The results show that the NC particle concentration has the most significant influence. As the NC concentration increases from 0.5% to 1.5%, the average Pc−c value sharply increases from approximately 6800 to 8400 N/mm². Lower concentrations resulted in smaller specific cutting forces, possibly because the hard and spherical Al_2O_3 nanoparticles could create a "rolling effect" to reduce friction and heat in the cutting zone. However, at higher concentrations, the nanoparticles tend to agglomerate into larger clusters, which in turn increases friction and impedes the cutting process. Additionally, the pressure air has a considerable effect on the specific cutting force. Increasing the pressure enhances the penetration of the nanofluid into the cutting zone, thereby improving cutting performance and causing a reduction in the specific cutting force. The specific cutting force reaches its minimum value at a pressure of approximately 5.5 bar and tends to increase as the pressure rises to 6 bar. This may be because excessive pressure can expel the nanofluid from the cutting zone, thus adversely impacting the cutting process.

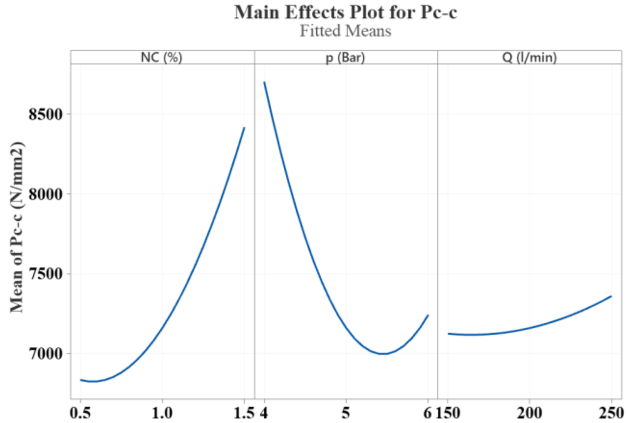

Fig. 3: *Influence of input factors on the specific cutting force*
"Source: Created by authors"

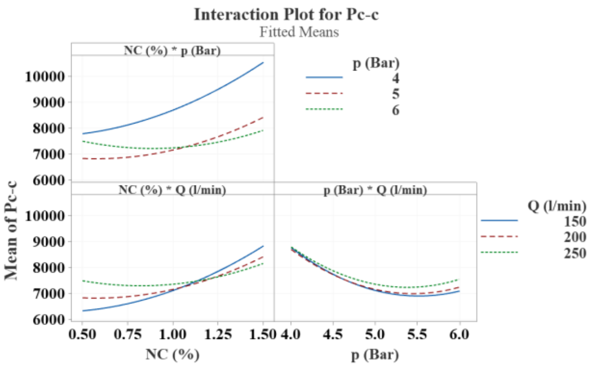

Fig. 4: *Interaction effects of input factors on the specific cutting force*
"Source: Created by authors"

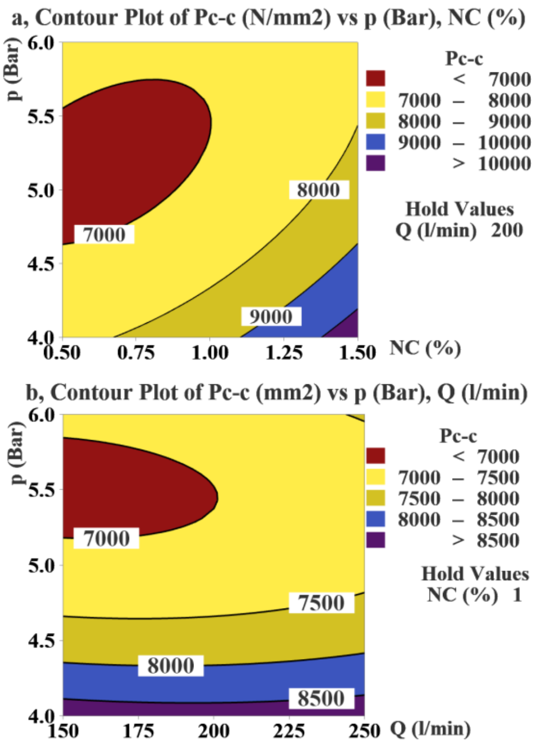

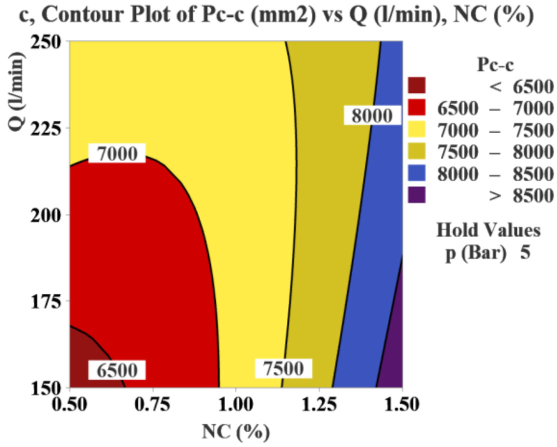

Fig. 5: *Contour plot of the effects of input factors on the specific cutting force*
"Source: Created by authors"

The interaction effects of the studied factors on the specific cutting force are illustrated in Figure 4. These results indicate the interdependent influence of NFMQL process parameters on the specific cutting force objective function (Pc−c). The results show that the second-order interaction between nanoparticle concentration (NC) and compressed air pressure (p) has a strong influence, while other interactions have a small influence on the Pc−c objective function. At low pressure (4 Bar), the energy of the air is not enough to push the nanofluid into the cutting zone. This causes the nanoparticles to agglomerate, increasing the viscosity and reducing the cooling lubrication efficiency, which in turn leads to a higher specific cutting force.As the pressure increases (5-6 Bar), spherical Al_2O_3 nanoparticles easily enter the cutting zone, providing superior lubrication. This significantly reduces the negative impact due to increased nanoparticle concentration. Compared to the NC*p interaction, the remaining interactions—between concentration and flow (NC*Q) and between pressure and flow (p*Q)—have a much weaker influence.

The interaction effects of the factors on the specific cutting force, Pc−c, are presented in more detail in the contour plots shown in Figure 5. The results show that at a flow rate of about 200 l/min, the specific cutting force reaches its minimum value when the concentration is in the range of 0.5-0.8%, and the air pressure is in the range of 4.5 to 5.5 bar. Based on the plots, to minimize the specific cutting force, at a fixed pressure p bar, the particle concentration should be kept below 1% and the flow rate below 200 l/min. When the particle concentration is fixed at 1%, the air pressure should be maintained at about 5.5 bar with the flow rate below 200 l/min.

3.3 Effect on the Active Cutting Force (Fa)

The influence of particle concentration, pressure, and air flow rate on the active cutting force (Fa) during the hard turning of steel using Al_2O_3 NFMQL technology is illustrated in Figure 6. Particle concentration and pressure are the two factors with the most significant impact on the active force Fa. As the NC concentration increases within the investigated range of 0.5% to 1.5%, the active force (Fa) correspondingly rises from approximately 101 N to a maximum value of 124N. This suggests that an increase in nanoparticle concentration within the NFMQL fluid heightens the resistive force during the cutting process, which may be attributed to changes in viscosity or the interactive properties of the fluid at the cutting zone. Meanwhile, the active force Fa tends to decrease as air pressure is increased from 4 to 5.5 bar, but the force increases again when the pressure is further raised to 6 bar. This can be explained by the fact that low air pressure will not have enough energy to push Al_2O_3 nanofluid into the cutting zone, while too high pressure will push it out of the zone. Therefore, it is important to determine the optimum pressure that is sufficient to maintain the required amount of nanofluid in the cutting zone, thereby improving the machining conditions. Furthermore, the influence of gas flow rate (Q) on the active cutting force is negligible compared to the other two factors.

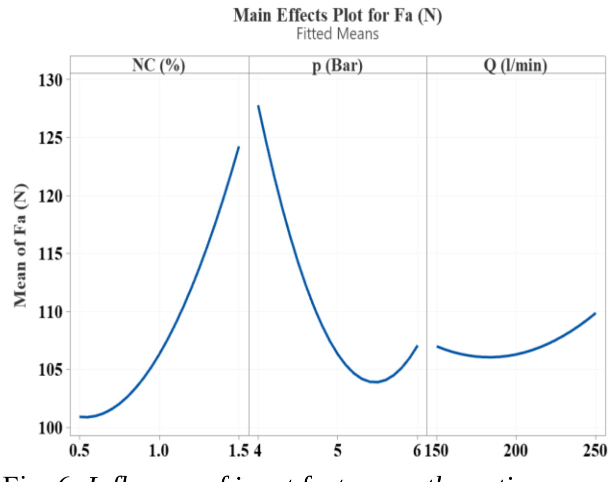

Fig. 6: *Influence of input factors on the active cutting force*
"Source: Created by authors"

Figure 7 illustrates the interaction effects of the studied factors on the active cutting force (Fa). The results show that the interaction between nanoparticle concentration and air pressure (NC*p) is statistically significant and has the most pronounced effect on the objective function Fa.

Other interactions have a minor effect on the active cutting force. These findings suggest that low air pressures (4 bar) should be avoided in machining with NFMQL technology. At low pressures (p = 4 Bar), the air flow energy is insufficient to disperse and drive the Al_2O_3 nano solution into the cutting zone. As a result, the lubricating "rolling effect" of the spherical nanoparticles is reduced. Instead, increasing the concentration (NC) at this pressure can increase the viscosity of the fluid and promote particle agglomeration - thereby increasing friction and leading to a strong increase in cutting force. Conversely, higher pressure levels (5 and 6 Bar) have been shown to facilitate the operation of the rolling lubrication mechanism, thus minimizing the adverse effects of increased nanoparticle concentrations.

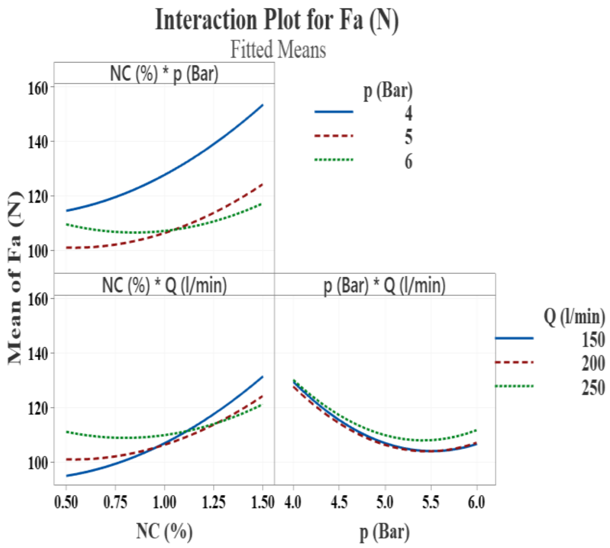

Fig. 7: *Interaction effects of input factors on the active cutting force*
"Source: Created by authors"

The contour plot for the active cutting force F_a (Figure 8) indicated that during the hard turning of 90CrSi steel using Al_2O_3 NFMQL, optimal parameters are achieved with an air flow rate below 200 l/min, an air pressure above 4.5 bar, and a nanoparticle concentration under 1.2%. The displayed results also confirm the dominant influence of concentration (NC) and pressure (p) on the active cutting force when compared to the flow rate (Q). The sensitivity of the Fa response to variations in NC and p is significantly higher than its sensitivity to Q.

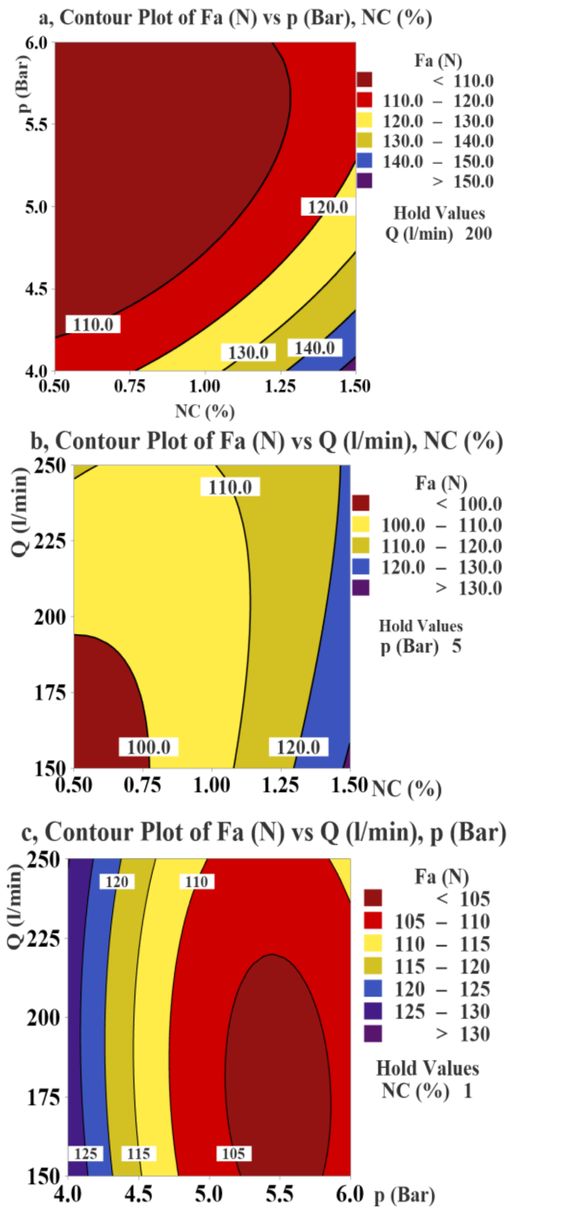

Fig. 8: Contour plot of the effects of input factors on the active cutting force
"Source: Created by authors"

3.4. Effect of the Technology Parameters of the NFMQL Method on the Passive Cutting Force (Fp)

The plot in Figure 9 reveals that the investigated factors (NC, p, and Q) significantly influence the passive cutting force, F_p. At a low concentration (0.5%), the quantity of nanoparticles is insufficient to form a stable lubricating film or to fully exhibit the "rolling effect", leading to high friction and consequently a large passive force. Conversely, at an excessively high concentration (1.5%), the nanoparticles tend to agglomerate, which diminishes their lubricating capability and can instead impede the cutting process, resulting in an increased passive cutting force. The results also suggest that the nanoparticle concentration should be maintained at approximately 1%, where lubrication efficiency is maximized, thus helping to reduce the passive force. However, the air pressure (p) tends to exert a linear influence on the passive cutting force. An increase in air pressure can cause nanoparticles to be wedged into the tool-workpiece contact zone, thereby increasing the passive force, F_p. Furthermore, the air flow rate (Q) also has a major influence on the force F_p, which tends toward its minimum value when the flow rate is around 200 l/min.

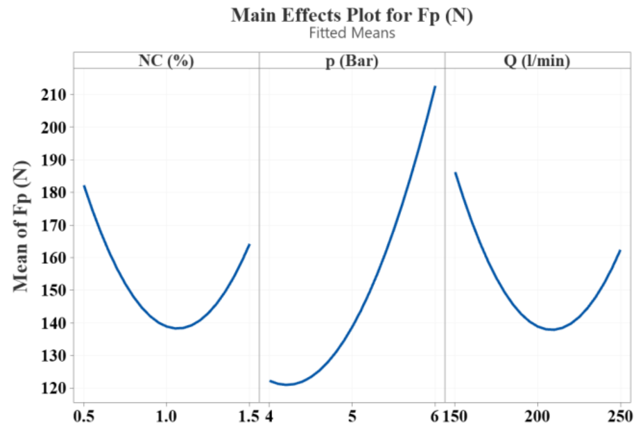

Fig. 9: *Influence of input factors on the passive cutting force*
"Source: Created by authors"

The plot in Figure 10 indicates that the interactions between Concentration & Flow Rate (NC*Q) and Pressure & Flow Rate (p*Q) strongly influence the passive cutting force. In contrast, the NC*p interaction has a weaker influence on the passive cutting force, F_p. At high flow rates (200 and 250 l/min), an increase in pressure causes the F_p force to rise sharply. Conversely, at a low flow rate (150 l/min), pressure has a negligible effect. Furthermore, the F_p force is at its minimum at a flow rate of 200 l/min and a concentration of approximately 1.0%.

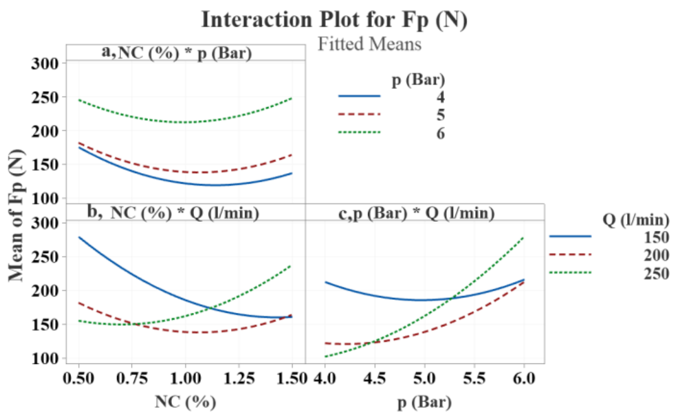

Fig. 10: *Interaction effects of input factors on the passive cutting force*
"Source: Created by authors"

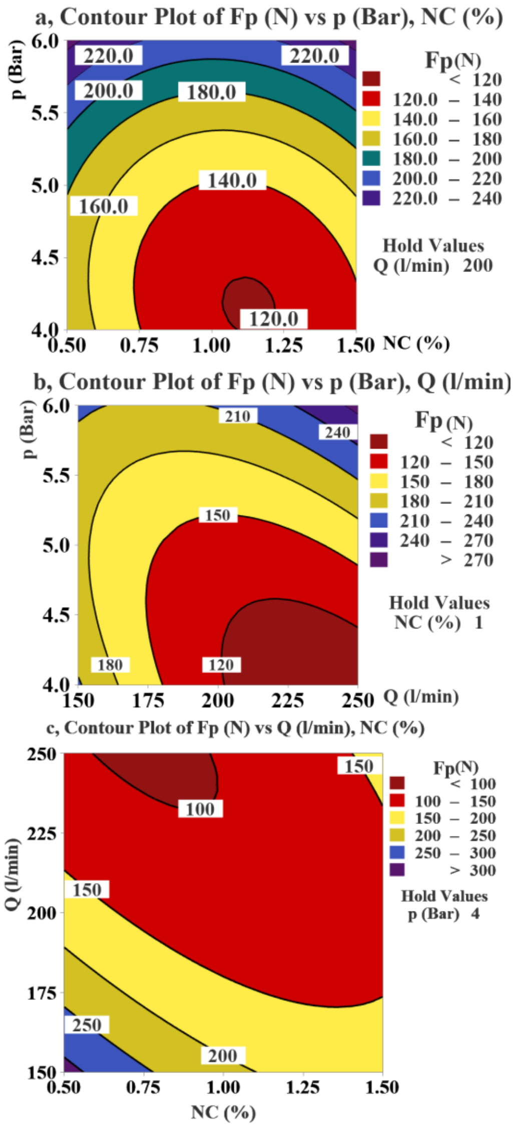

Fig. 11: *Contour plot of the effects of input factors on the passive cutting force*
"Source: Created by authors"

The interaction effects between the factors are detailed further in the contour plots presented in Figure 11. The results indicate that at a fixed concentration of 1% (Figure 11a), a low cutting force is achieved when using low air pressure in combination with a high air flow rate. Furthermore, at a constant flow rate of 200 l/min (Figure 11b), a particle concentration of approximately 1-1.25% and a pressure below 5 bar should be utilized to maintain a cutting force of less than 140N. Figure 11c shows that with the pressure fixed at 5 bar, a low cutting force can be obtained by either increasing the particle concentration while decreasing the flow rate, or vice versa, indicating a trade-off between these two parameters.

3.5. Determination of Optimal Process Parameters

The optimal set of process parameters was determined using the Response Optimizer module in the Minitab 21 software, with the results presented in Figure 12, Figure 13, Figure 14, and Figure 15. Figure 12 displays the optimization results for the specific cutting force, $P_{c\text{-}c}$. A minimum specific cutting force of $P_{c\text{-}c}$ = 6322.75 N/mm² is achieved with the parameters: NC = 0.5%, p ≈ 5.15 Bar, and Q = 150 l/min.

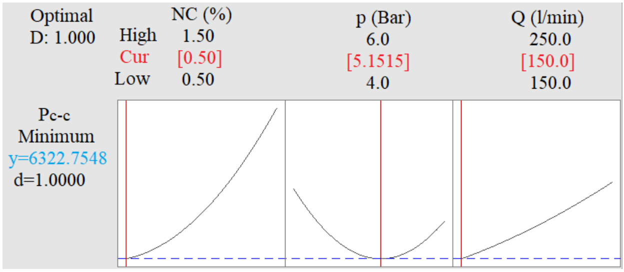

Fig. 12: *Optimization of the specific cutting force P_{c-c}.*
"Source: Created by authors"

The optimization results for the active cutting force, F_a, are presented in Figure 13. According to the developed predictive model, a minimum active cutting force of 94.7 N is achieved with the following parameter set: NC = 0.5%, p ≈ 5.21 Bar, and Q = 150 l/min.

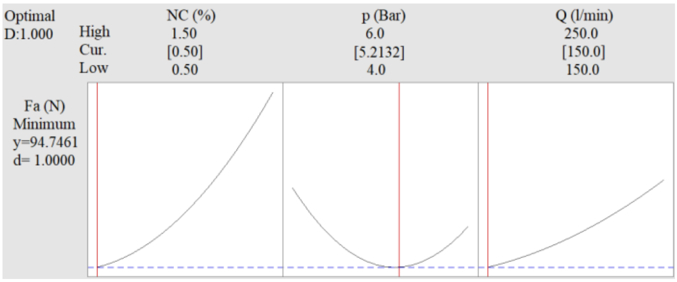

Fig. 13: *Optimization of the active cutting force F_a*
"Source: Created by authors"

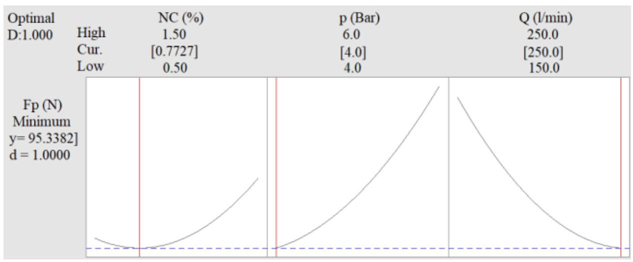

Fig. 14: *Optimization of the passive cutting force Fp.*
"Source: Created by authors"

The optimization analysis indicates that a specific combination of process parameters can be identified to minimize the passive cutting force (F_p). Based on the regression model, the predicted minimum F_p value is 95.34 N, which is achieved with the following parameters: Concentration (NC)-0.77%, Pressure (p) 4.0 Bar, Flow Rate (Q) 250.0 l/min.

A multi-objective optimization analysis was performed to identify a set of process parameters capable of simultaneously minimizing all three responses: the active cutting force (F_a), the specific cutting force (P_{c-c}), and the passive cutting force (F_p). The results, displayed in Figure 15, show a Composite Desirability of D = 0.8376. Although this value is less than 1, it represents a strong compromise solution, which is necessary due to the conflicting requirements among the output responses. The proposed optimal parameter set is NC ≈ 0.79%, p ≈ 4.97 Bar, Q ≈ 205.6 l/min. Under these conditions, the predicted values for the responses are F_a = 103.27 N, P_{c-c} = 6962.2 N/mm², and F_p = 143.95 N.

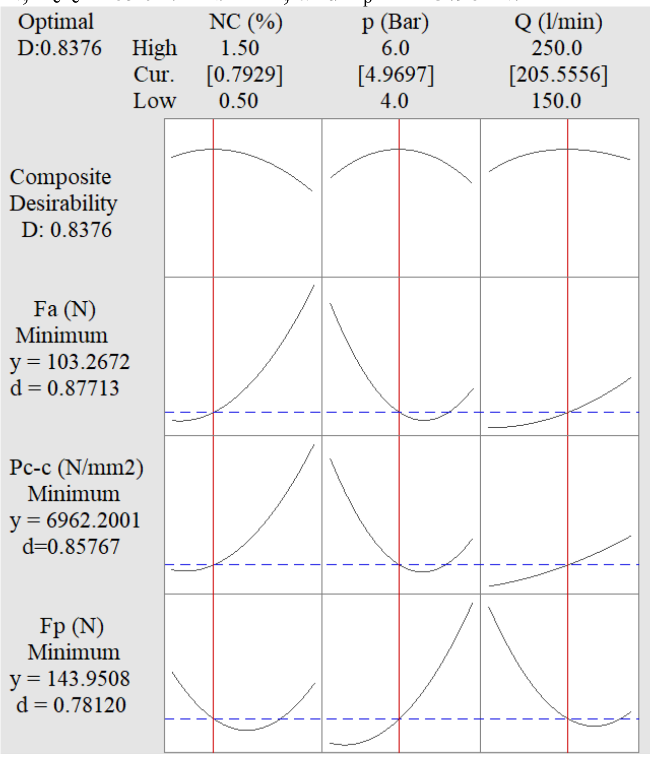

Fig. 15: *Multi-objective Optimization.*
"Source: Created by authors"

Table 6. *Summary of optimization results*

Obj. Fun.	**NC (%)**	**p (Bar)**	**Q (l/min)**	**Pc-c (N/mm2) Min.**	**Fa(N) Min.**	**Fp(N) Min.**	**D**
P_{c-c}	0.5	5.15	150	6322.7	-	-	1.0
F_a	0.5	5.2	150	-	94.7	-	1.0
F_p	0.77	4.0	250	-	-	95.3	1.0
P_{c-c}, F_a, F_p	0.79	4.97	205.6	6962	103.2	143.9	0.8376

"Source: Created by authors"

Table 6 summarizes the optimization results for different objective functions in hard turning processes using MQL NF Al_2O_3 technology. These optimization results, combined with the contour plots (Figure 5, Figure 8 and Figure 11), help engineers choose appropriate NFMQL technology parameters in actual production.

4 Conclusion

This study analyzed the effects of nanoparticle concentration (NC), pressure (p) and gas flow rate (Q) on three cutting force components (F_a, F_p, P_{c-c}) during hard turning of 90CrSi steel using the NFMQL method. The results showed that the active cutting force (F_a) and specific cutting force (P_{c-c}) were most significantly influenced by concentration and pressure, with optimal values achieved at low concentration and medium pressure (approximately 5.2 Bar). In contrast, the passive cutting force (F_p) was strongly influenced by the interaction between the factors and this interaction effect also decreased at low pressure (4.0 Bar). To ensure the simultaneous achievement of the objectives, a compromise solution was identified. The overall optimal parameter set proposed was NC ≈ 0.79%, p ≈ 4.97 Bar and Q ≈ 205.6 l/min. Under these conditions, the cutting force components do not reach absolute minimum values, but the best overall balance is maintained. In practical terms, by adopting these settings, manufacturing facilities can achieve a reliable balance: maintaining high cutting performance (represented by controlled active and specific forces) while ensuring high machining accuracy (by controlling passive forces, which cause dimensional errors). This brings tangible benefits such as increased productivity, reduced tool wear and reduced scrapping, which directly contribute to reduced operating costs and improved product quality in the mold and die industry, where 90CrSi steel is very popular.

Acknowledgement:
The study had the support of Thai Nguyen University of Technology, Thai Nguyen University.

References:

[1] J. P. Davim and V. P. Astakhov, *Machining of Hard Metals*, Springer London 2011, https://doi.org/10.1007/978-1-84996-450-0

[2] Manjunath Patel G. C, Ganesh R. Chate, Mahesh B. Parappagoudar, Kapil Gupta (2020), *Machining of Hard Materials, A Comprehensive Approach to Experimentation*, Modeling and Optimization, Springer, https://doi.org/10.1007/978-3-030-40102-3

[3] Syed Hammad ALI, Yu YAO, Bangfu WU, Biao ZHAO, Wenfeng DING, Muhammad JAMIL, Ahmar KHAN, Asra BAIG, Qi LIU, Dongdong XU, *Recent developments in MQL machining of aeronautical materials: A comparative review*, Chinese Journal of Aeronautics, Available online 20 January 2024, https://doi.org/10.1016/j.cja.2024.01.018

[4] Tao He, Niancong Liu, Huazheng Xia, Long Wu, Yu Zhang, Daigang L, Yun Chen, *Progress and trend of minimum quantity lubrication (MQL): A comprehensive review*, Journal of Cleaner Production, Volume 386, 1 February 2023, https://doi.org/10.1016/j.jclepro.2022.135809

[5] Sharma A.K., Tiwari A.K., Dixit A.R., *Effects of Minimum Quantity Lubrication (MQL) in machining processes using conventional and nanofluid-based cutting fluids: A comprehensive review*, Journal of Cleaner Production 2016, 127, 1-18, https://doi.org/10.1016/j.jclepro.2016.03.146

[6] Arumugam Balasuadhakar, S. Thirumalai Kumaran, Farooq Ahmed, *A review on the role of nanoparticles in MQL machining*, Materials Today: Proceedings, Volume 72, Part 6, 2023, Pages 2828-2832, https://doi.org/10.1016/j.matpr.2022.07.247

[7] S. S. Rahman, M. Z. I. Ashraf, A. K. M. N. Amin, M. S. Bashar, M. F. K. Ashik, M. Kamruzzaman, *Tuning nanofluids for improved lubrication performance in turning biomedical grade titanium alloy*, J Clean Production, vol. 206, pp. 180–96, 2019. https://doi.org/10.1016/j.jclepro.2018.09.150

[8] Leong K.Y., Ahmad K.Z.K., Ong H.C., Ghazali M.J., Baharum A., *Synthesis and thermal conductivity characteristic of hybrid nanofluids – A review*, Renewable and Sustainable Energy Reviews 2017, 75, 868-878, DOI: https://doi.org/10.1016/j.rser.2016.11.068

[9] Hegab, H., Umer, U., Soliman, M., Kishawy, H.A., *Effects of nano-cutting fluids on tool performance and chip morphology during machining Inconel 718*, The International Journal of Advanced Manufacturing Technology 2018, 96 (9–12), 3449–58, https://doi.org/10.1007/s00170-018-1825-0

[10] C. Darshan, S. Jain, M. Dogra, M. K. Gupta, M. Mia, *Machinability improvement in Inconel-718 by enhanced tribological and thermal environment using textured tool*, Journal of Thermal Analysis and Calorimetry, vol. 138, no. 1, pp. 273–285, 2019. https://doi.org/10.1007/S10973-019-08121-Y

[11] Gupta, M.K., Jamil M., Wang X.J., Song Q.H., Liu Z.Q., Mia M., *Performance evaluation of vegetable oil-based nano-cutting fluids in environmentally friendly machining of Inconel-800 alloy*, Materials 2019, 12 (17), 2792, https://doi.org/10.3390/ma12172792

[12] Zhang Y., Li C., Jia D., Zhang D., and Zhang X., *Experimental evaluation of MoS2 nanoparticles in jet MQL grinding with different types of vegetable oil as base oil*, Journal of Cleaner Production 2015, 87, 930–940, doi: https://doi.org/10.1016/j.jclepro.2014.10.027

[13] V. C. Nguyen, T. D. Nguyen, and D. H. Tien, *Cutting Parameter Optimization in Finishing Milling of Ti-6Al-4V Titanium Alloy under MQL Condition using TOPSIS and ANOVA Analysis*, Engineering, Technology & Applied Science Research, vol. 11, no. 1, pp. 6775–6780, Feb. 2021. https://doi.org/10.48084/etasr.4015

[14] Uysal A., Demiren F., and Altan E., *Applying Minimum Quantity Lubrication (MQL) Method on Milling of Martensitic Stainless Steel by Using Nano MoS2 Reinforced Vegetable Cutting Fluid*, Procedia - Social and Behavioral Sciences 2015, 195, 2742–2747, doi: https://doi.org/10.1016/j.sbspro.2015.06.384

[15] Yücel A., Yıldırım Ç.V., Sarıkaya M., Şirin Ş., Kıvak T., Gupta, M.K., İtalo V.T., *Influence of MoS2-based nanofluid-MQL on tribological and machining characteristics in turning of AA 2024 T3 aluminum alloy*, Journal of Materials Research and Technology 2021, 15, 1688–1704. https://doi.org/10.1016/j.jmrt.2021.09.007

[16] Rahmati B., Sarhan A. A. D., and Sayuti M., *Morphology of surface generated by end milling AL6061-T6 using molybdenum disulfide (MoS2) nanolubrication in end milling machining*, Journal of Cleaner Production, 2014, 66, 685–691, doi: https://doi.org/10.1016/j.jclepro.2013.10.048

[17] Wei Li, Zhixiong Zeng, ShaJiu Le, Keyi Zhu, Xiangming Huang, Hussien Hegab, Ahmed Mohamed Mahmoud Ibrahim, *Investigation of a green nanofluid added with graphene and Al2O3 nano-additives for grinding hard-to-cut materials*, Tribology International, Volume 195, July 2024, 109580, https://doi.org/10.1016/j.triboint.2024.109580

[18] Saurabh Tiwari, M. Amarnath, Munish Kumar Gupta, Munish Kumar Gupta, *Synthesis, characterization, and application of Al2O3/coconut oil-based nanofluids in sustainable machining of AISI 1040 steel*, Journal of Molecular Liquids, Volume 386, 15

September 2023, 122465, https://doi.org/10.1016/j.molliq.2023.122465

[19] K. Venkatesan, Arun Tom Mathew, S. Devendiran, Nouby M Ghazaly, S. Sanjith, R. Raghul, *Machinability study and multi-response optimization of cutting force, Surface roughness and tool wear on CNC turned Inconel 617 superalloy using Al2O3 Nanofluids in Coconut oil*, Procedia Manufacturing, Volume 30, 2019, Pages 396-403, https://doi.org/10.1016/j.promfg.2019.02.055

[20] Park K.-H., Olortegui-Yume J. A., Joshi S., Kwon P., Yoon M.-C., Lee G.-B., & Park S.-B, *Measurement of Droplet Size and Distribution for Minimum Quantity Lubrication (MQL)*, International Conference on Smart Manufacturing Application 2008, doi: https://doi.org/10.1109/ICSMA.2008.4505598

Contribution of Individual Authors to the Creation of a Scientific Article (Ghostwriting Policy)

The authors equally contributed to the present research, at all stages from the formulation of the problem to the final findings and solution.

Sources of Funding for Research Presented in a Scientific Article or the Scientific Article Itself

No funding was received for conducting this study.

Conflict of Interest

The authors have no conflicts of interest to declare that are relevant to the content of this article.